Adaptive Sum of Markov Chains for Modelling 3D Blockage in mmWave V2I Communications

Adaptive Sum of Markov Chains for Modelling 3D Blockage in mmWave V2I Communications

Fahd Alsaleem[‡*], John S. Thompson[*], and David I. Laurenson[*]
[‡]Department of Electrical Engineering, College of Engineering, Qassim University, Unaizah, Saudi Arabia
[*] Institute for Digital Communications (IDCOM), School of Engineering, The University of Edinburgh, Edinburgh EH9 3JL, U.K.
Emails: F.Alsaleem@ed.ac.uk, John.Thompson@ed.ac.uk, Dave.Laurenson@ed.ac.uk

***Abstract*—Blockage attenuation is one of the main challenges that face reliable communication at the millimetre-wave (mmWave) band, especially for dynamic vehicle-to-infrastructure (V2I) communication systems. Modelling the dynamics of the blockage is important for evaluating high gain beamforming techniques, which are used to improve the signal strength in the mmWave communication systems. The novel sum of Markov chains (sum of MC) model is designed to do two main tasks successfully; capturing the dynamics of blockers affecting a moving transceiver and computing the arising channel attenuation. The sum of MC model has advantages over existing Markov chains models, which are: that it can adapt to model non-stationary scenarios. The sum of MC model can integrate any attenuation function, including the 3GPP blockage model and any lab measurement attenuation profile. Additionally, it is computationally efficient. The sum of MC model can match well with the performance results from a more complex geometric channel model.**

***Index Terms*—mmWave, V2I, Markov Chain, Sum of Markov Chains, 3D blockage, 3GPP, METIS, Knife-edge diffraction**

I. Introduction

FUTURE vehicle communication systems require ultra-low latency and a high data rate for safety and service quality reasons. The millimetre-wave (mmWave) band with a frequency range from 30 GHz to 300 GHz has significant potential to achieve these target requirements since it can provide very wide bandwidth, enabling high data rate (gigabits/s), and ultra-low latency applications [1]. Despite these attractive features of the mmWave band, several challenges need to be addressed. Alongside the fact that the mmWave band suffers from a higher path loss than lower frequency microwave bands, attenuation due to blockage from an obstacle crossing the line of sight (LOS) path is another major issue [2], [3]. For instance, the human body attenuates the mmWave signal in the range from 20 to 25 dB [4]. At mmWave frequencies, the diffraction of electromagnetic waves around blockers (BL) is less likely to occur than at microwave frequencies due to the significant difference in the size of a typical blocker and the wavelength [5], so even small obstacles can influence the signal strength [6]. The probability of LOS blockage increases exponentially as the receiver moves further away from BS [7].

The following subsections present: a brief overview of the related work; outlining the main contributions of the paper, and then the structure of the paper.

A. Related Work

In this subsection, we have grouped the existing studies into four categories: first, discussing the impact of the blockage on the channel and how important understanding blockage behaviour is. Second, the frequency ranges of the mmWave band are investigated. Then, how blockage effects have been modelled is presented in the literature review. Finally, a succinct overview of the existing works that use a Markov chain to model blockage events is outlined.

1) The importance of understanding the dynamic blockage effect on the mmWave channel: The rapid change in the signal strength due to blockages will cause a sudden change to the channel attenuation. Dynamic blockages, such as moving people, cars, and buses, cause rapid fluctuations in the mmWave channel, leading to rapid reductions in the signal strength of up to 30-40 dB [8]. Therefore, accurate modelling of the dynamics of blockage is essential for developing reliable transceivers for mmWave systems [9]. The authors of [9] introduce a novel spatial dynamic channel sounding system at a frequency of 60 GHz. Moreover, based on the results in [10], [11], the authors propose that dynamic blockage plays an important role in the engineering design of mmWave cellular systems. Blockages impact on the channel propagation and on achieving the optimum antenna configuration for a given environment [12]. Understanding the behaviour of dynamic blockages could provide an important assessment of the future fully adaptive beamforming. Reference [13] states that the process of environment digitalization is one of the factors that will enable advanced beamforming approaches. They used ray-tracing tools to investigate pencil-beam forming techniques assuming full knowledge of the channel characteristics. Thus, we believe that a more in-depth understanding of dynamic blockage behaviour in directional mmWave communications, especially in V2I communication, would help to improve the overall quality of service of the mmWave system. Reference [14] analyses the effect of blockage on the relationship between the blockage rate and the data frame length. Reference [15] studied using their novel model the behaviour of correlation between the LOS path and the reflected paths that are affected by human blockage around receivers. However, they have avoided using the 3GPP blockage model to reduce complexity; instead, they assumed that each blocker introduces a fixed 20 dB loss.

2) Frequency ranges investigated: The impact of human blockage on 60 GHz band has attracted many research endeavours in the early literature based on the IEEE 802.11ad standard. For instance, reference [16] studied outdoor scenarios, and [4], [17], [18] have investigated the indoor environment. Reference [19] has provided analysis and comparisons between different blockage models at 60 GHz. It states that even clothes have a significant impact on the resulting attenuation under some circumstances. Other studies investigate the influence of human blockage at other frequency ranges of 28 GHz [20] and the 73 GHz band was investigated by some studies in [21] and [22]. Also, the human blockage effect at 28 GHz, 38 GHz, 60 GHz, and 73 GHz frequency bands were studied in [23], which concludes that 28 GHz showed a lower blockage loss compared with the other frequency bands. Reference [22] shows that using directional antennas, one human blocker could attenuate the signal by 30-40 dB. Also, the 11, 16, 28 and 32 GHz bands are studied in [24]. The paper states that increasing the frequency within this range would have no significant influence on the attenuation value.

3) How have human blockers been modelled in the literature?: Two main steps are required in blockage modelling. The first is determining the blocker location: distributing blockers uniformly over the area around the base station (BS) and the receiver (RX) is a well-known approach e.g. see [14]–[16], [25]. The second step is to model the attenuation profile caused by a given blocker. For the mmWave band, several approaches have been undertaken by researchers to model the attenuation caused by a human blockage. Below, the main approaches are briefly outlined and listed in increasing order of complexity:

1) A simple approach [16], [26] is to have a fixed attenuation where each human blockage introduces a fixed attenuation of 20 dB, which is based on experimental results.
2) Modelling a blocker as a screen and then applying knife-edge diffraction theory to get the attenuation value is a common approach in the literature. In the METIS channel models [27], simple knife-edge diffraction is used to calculate the loss value geometrically. This is one of two empirical-based blockage models proposed by the 3GPP standards body [28]. Several other studies use double-sided knife-edges and examine it with some measurements, such as [22]. Their results show that using a directional antenna, one human blocker could attenuate the signal by 30-40 dB when the TX-RX distance is 5m. Reference [29] also introduces some basic rules to use the simplified double knife-edge to model human blocker effects in the mmWave band.
3) Other geometric approaches are used to model a blockage, such as the Kirchhoff KED model and the geometrical theory of diffraction in (GTD) [24]; and the circular cylinder, dielectric elliptic cylinder, and multiple knife-edge diffraction in [19]. However, these models are much more complex to evaluate.

4) Markov Chain Blockage Models: Modelling the blockage event using the Markov chain is not a new concept. A simple two-state Markov model has been used in several studies in the literature; the author of [30] introduces a two-state Markov chain approximation, using fade and non-fade states, for slow Rayleigh fading channels. Likewise, reference [31] uses two-state Markov, shadowed and non-shadowed states, to capture the blockage for indoor populated environments. Reference [21] developed two approaches using a Markov model for modelling the blockage event: a two-state Markov chain and a four-state piecewise linear modelling approach. These are used to model a human blocker in an outdoor environment where there is only a single TX-RX LOS. Moreover, reference [32] defines a Markov model with three states: non-line of sight (NLOS), line of sight (LOS) and no signal. Reference [33] extracted transition probabilities of the evolution in the line of sight (LOS) blockage of the V2V system using a three-state Markov chain with actual measurements of different environments. However, the frequency band used was between 2 GHz and 6 GHz, rather than considering mmWave frequencies. In earlier work [26], we also propose a Markov chain model to capture blockage densities surrounding a moving vehicle where each state represents the number of blockers that intersect with the LOS path. However, this work has some limitations that are indeed addressed in this current paper's approach, which will be discussed further below. Investigating the effect of blockage on the V2I links at mmWave frequencies thus requires further research.

B. The Main Contributions

To the best of our knowledge, capturing the dynamic of the blockers surrounding a moving transceiver, and at the same time computing the resulting attenuation has not been studied in the literature. This study investigates blockage effects on the signal strength and captures the dynamics of blockers surrounding a moving transceiver.

1) A novel sum of Markov chains (sum of MC) model is proposed that successfully captures the dynamics of the blockage surrounding a moving transceiver that moves around a base station. Moreover, the performance of the proposed model shows a very good match with the geometric model results, but with much less complexity. The simplicity of the proposed model is a very good feature; it is based on several two-state Markov chains combined in parallel. To estimate the right average number of blockers for any given environment, the only three inputs required for the model are the right choice of the transition probability, the length of a blocker, and how many chains are required.
2) One of the advantages of the proposed sum of MC model is that it can work very well for both stationary and non-stationary scenarios; non-stationary means the average number of blockers can vary depending on the TX-RX distance and the blocker locations since the probability of LOS blockage increases exponentially with TX-RX distance [7]. This is due to the adaptive feature of the proposed model, which can adapt and predict the correct dynamics of the average number of blockers for any given environment.
3) To add more novelty to the work, any attenuation model could be integrated easily within the novel proposed sum

of MC model. One of the blockage models that could be used is the third-generation partnership project (3GPP) knife-edge diffraction (KED) blockage model; in this paper, it is adopted and integrated within the proposed model. Thus, the resulting attenuation of the model is not only based on how many blockers there are but also on the relative locations of these blockers.

C. Paper Organisation

The paper is organised as follows: in Section II the system model of the paper and propagation scenarios are presented. Then, Section III presents two possible approaches to compute the attenuation value caused by blockers. Both approaches will be used later on the paper. In this section, the 3GPP blockage model is adopted to represent the second approach, along with an attenuation profile of RF lab measurements. Then, in the following section, state of the art blockage models – geometric, and Markov chain – are introduced with a brief overview of the initial work in [26]. Section V comprises the core of the paper, where the novel sum of Markov chains (sum of MC) model is proposed. Section VI provides results and discussion of all the models. Section VII shows a summary of the work, highlights the main achievements, and suggests possible directions for future work. The last section provides a link to the MATLAB code used in this paper.

II. The System Model

To investigate the blockage effect on the mmWave V2I communication system, in the proposed system model we assume that there is a mobile transceiver at the top of a vehicle that is moving around a base station in the presence of a sparse distribution of blockers located randomly in the area. Since in the mmWave band the line-of-sight (LOS) path is far stronger than other non-LOS paths [34], we only consider the LOS path in this paper. Whenever the LOS path hits a blocker, attenuation is applied in the model. As in [16], we assume the angle of arrival does not change. In the following subsections, the geometric model parameters and the theoretical approach for computing the average number blockers are defined. Then, propagation scenarios are introduced to investigate how much a blocker could affect the received signal strength. Finally, since the channel capacity is simple to compute, we use it as a metric to compare the performance of different approaches to model blockage.

A. Introducing the system model parameters

The system model, as shown in Fig. 1(a), consists of a base station (BS), with height h_T, and a mobile transceiver (MT), with height h_R, moving around the BS following a specified track. For simulation purposes, there are N sample points that are equally spaced and located on the track. The MT starts moving at sample point 1 and finishes at sample point N, with corresponding sample times t_1 to t_N. Within the area A_T, there are N_{BL} blockers that could block the LOS path between the BS and the MT. Any blocker shape could be used; the blocker radius is defined as r_{BL} and the height is h_{BL}. If

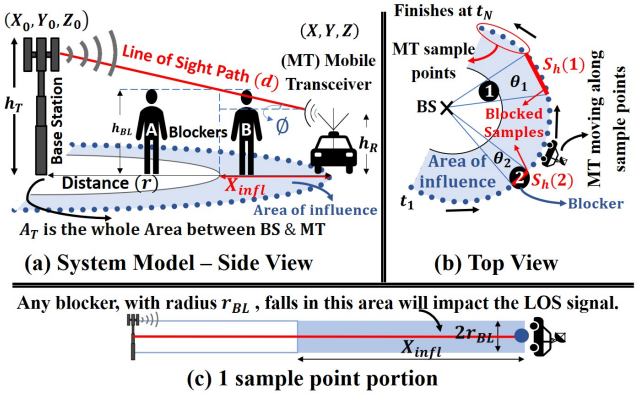

Fig. 1. The System Model.

a signal passes through any one of these blockers, its power will be significantly reduced. The more blockers, the greater the overall attenuation the signal experiences. Since the BS is assumed to be higher than the blockers, only the blockers that cross the LOS signal path are counted, such as blocker B in Fig. 1(a), while blocker A would not have any effect. Therefore, this only refers to the blockers located within the area of influence, which is where the direct LOS path does not exceed the height of a blocker h_{BL}. The scalar X_{infl} is the distance between the two edges of the influence-ring in Fig. 1(a) and it is found from the elevation angle ϕ of the LOS path as follows:

$$\tan\phi = \frac{(h_T - h_R)}{r} = \frac{(h_{BL} - h_R)}{X_{infl}} \tag{1}$$

$$X_{infl} = r\frac{(h_{BL} - h_R)}{(h_T - h_R)} \tag{2}$$

The scalar d is the length of the LOS path from the BS at coordinates (X_0, Y_0, Z_0) to the MT sample point (X, Y, Z). The average number of blockers at each sample point is obtained by multiplying the blocker density by the area of visibility of this sample point, as shown in Fig. 1(c), which is a slight modification of what was shown in [26]. It is calculated as follows:

$$N_G^{'} = \varepsilon(2r_{BL}X_{infl}) \tag{3}$$

where $\varepsilon = \frac{N_{BL}}{A_T}$ is the average number of blockers per unit area, i.e. the blocker density, and N_{BL} is the total number of blockers that exist in area A_T. The scalar r_{BL} is the radius of one blocker.

As in [14]–[16], [25] blockers are uniformly distributed, and they can be located anywhere in area A_T. However, the shadow caused by a blocker projection on the MT track will vary based on the blocker location. Fig. 1(b) shows that a blocker (No. 1) that is far from the MT track will create a longer shadow on the MT track with length $S_h(1)$. A shorter shadow area with length, $S_h(2)$, on the other hand, will be created by a blocker located very close to the MT track, (No. 2). These are the two extreme cases of the blocker location.

The scalar $S_h(1)$ is found by applying the arc length formula as follows:

$$\tan\theta_1 = \frac{(2r_{BL})}{r - X_{infl}} = \frac{S_h(1)}{r} \Rightarrow S_h(1) = \frac{(2r_{BL})r}{r - X_{infl}} \quad (4)$$

Similarly, for blocker No. 2 located on the MT track, the projected sector equals the diameter of the blocker, i.e. $Sh(2) = 2r_{BL}$. The average shadow-length, $\overline{Sh}$, caused by one blocker is obtained from integrating over all possible blocker locations, which yields the average length as:

$$\begin{aligned}\overline{Sh} = \mathbb{E}(Sh) &= \int_{S_h(2)}^{S_h(1)} \frac{x}{S_h(1) - S_h(2)} dx \\ &= \frac{(S_h(1))^2 - (S_h(2))^2}{2(S_h(1) - S_h(2))} = \frac{S_h(1) + S_h(2)}{2} \\ &= r_{BL}\left(\frac{r}{r - X_{infl}} + 1\right) \quad \text{(m)}\end{aligned} \quad (5)$$

However, by dividing the number of sample points over the total length of the mobile transceiver track, we get the number of samples per unit length, i.e. N/L. Thus, the average number of sample points that is affected by one blocker is obtained by multiplying (6) by N/L as follows:

$$l_B = \overline{Sh}\frac{N}{L} = \frac{Nr_{BL}}{L}\left(\frac{r}{r - X_{infl}} + 1\right) \quad \text{(Samples)} \quad (6)$$

In this paper, we assume a sparse distribution of the blockers, where the total blocker length or breadth is much less than the BS-MT distance. As stated in the METIS model [27], for sparsely populated environments, when the shadow of two different blockers overlap, the net overall attenuation is the sum of the attenuation values (in dB) for each blocker. The computation of blocker attenuation is explained in detail in Section III.

B. Propagation scenarios

As noted at the start of this section, we only consider the LOS path in this paper. Thus, similar to [35] one of two cases is possible; the LOS path is either non-blocked or blocked:

1) LOS Propagation: when no blocker crosses the LOS path between the BS and the MT, the Friis equation of the received power [36] can be written as a function of the antennas' directivity, D_T and D_R, and the free-space path-loss, $P_L = (4\pi d/\lambda)^2$. The wavelength, λ, is much smaller than the direct LOS path, d, i.e. the far-field assumption is made.

$$P_R(t) = \frac{P_T(t)D_T D_R}{P_L} \quad \text{(W)} \quad (7)$$

2) Blocked LOS Propagation: in the presence of blockers, since the attenuation that each blocker causes P_{BL} is known, this can be added to (7). The received LOS signal in (7) will be partially blocked and hence suffer from unit power Rayleigh fading due to the blocker effect, with power equal to $|R^2|$, where $|R|$ is the Rayleigh fading amplitude. Equation (8) is only considered when the signal passes through one or more blockers, i.e. $N_G^{'} \geqslant 1$:

$$P_R(t) = \frac{P_T(t)D_T D_R|R^2|}{P_L N_G^{'} P_{BL}} \quad \text{(W)} \quad (8)$$

C. Channel Capacity

Thanks to the well-known Shannon equation [37], the maximum spectral efficiency at each sample point can be obtained easily using the resulting received power as in (9). The channel capacity will be used later to compare the performance of different blockage models.

$$C(t) = \log_2\{1 + P_R(t)/N_o\} \quad \text{(bits/s/Hz)} \quad (9)$$

We used the channel capacity as a metric to evaluate the proposed model. We know that the Shannon capacity is an upper-bound, and actual system performance should be below that. However, reference [38] has shown that the Long Term Evolution (LTE) link capacity curve is close to the Shannon upper-bound with only a small difference. Hence, the Shannon equation provides a good way to approximate the performance of real systems using adaptive modulation and coding.

III. Blockage Attenuation Approaches

When a blocker crosses the direct path between a transmitter and a receiver, it attenuates the signal and makes it weaker. The resulting attenuation depends on the blocker's kind, size, location, and orientation. As mention in Section I-A, several approaches have been undertaken by researchers to evaluate the attenuation caused by a human blockage. In this paper, we consider two approaches listed in increasing order of complexity. Moreover, towards the end of this section, an attenuation profile of lab measurements is presented, which could be used as well.

A. Approach (1): Fixed-Attenuation Blockage Model

For the mmWave band, if a signal passes through one human blocker, its power will drop roughly by 20 dB [4]. This simple approach involves introducing a 20 dB fixed attenuation value whenever the LOS path is blocked.

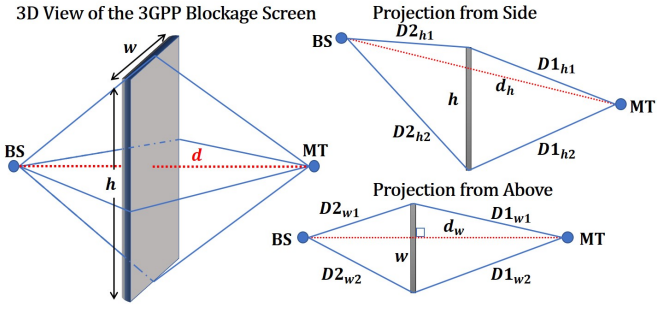

Fig. 2. Shadowing screen model adopted from [27], and [28].

B. Approach (2): 3GPP Blockage Model

In principle, not every human body that crosses the LOS path should attenuate the signal by a fixed value of 20 dB. The attenuation of a blocker will vary depending on the location and the orientation. However, 3GPP provides a simple model to capture the loss caused by the shadow of a blocker using the concept of knife-edge diffraction [27], [28]. Each blocker

is represented by a rectangular screen, as in Fig. 2, and the loss due to four edges of the screen is:

$$P_{BL} = -20\log_{10}\left(1-\left(F_{h1}+F_{h2}\right)\left(F_{w1}+F_{w2}\right)\right)\ (\mathrm{dB}) \tag{10}$$

where F_{h1}, F_{h2}, F_{w1}, and F_{w2} are the diffraction values associated with the four edges; h denotes the blocker height and w the width, as shown in Fig. 2. Every edge will cause shadowing equal to:

$$F = \frac{\operatorname{atan}\left(\pm\frac{\pi}{2}\sqrt{\frac{\pi}{\lambda}\left(\mathrm{D}_1+\mathrm{D}_2-\mathrm{d}\right)}\right)}{\pi} \tag{11}$$

where λ is the wavelength, D_1 and D_2 are the projected distance from the BS and MT nodes to the screen, and d is the projected distance between the BS and MT nodes.

According to [27], [28], when one of the BS or MT nodes moves, the orientation of the screen should be rotated around its centre to be perpendicular to the LOS path, and at the same time stay vertical on the ground. Thus, if we look at this from the top view, the cross-section of the rotation makes a circular shape that has a diameter equal to the 3GPP screen width. This is not a cylinder, just a screen that rotates around its centre to always be perpendicular to the LOS path.

This 3GPP blockage model is adopted in this paper. Whenever a blocker crosses the LOS path, the above loss equation is applied to obtain the attenuation caused by that blocker. The attenuation value will vary depending on the blockage location. This 3GPP blockage model can be used in the geometric model and the sum of MC model, but not the Markov chain model; that is explained in detail in the next section, in Section IV-B.

According to the METIS project [27], and the 3GPP standard body [28], for a sparse distribution of blockers, when the shadow of two blockers overlapped, each one will attenuate the signal separately. The resulting attenuation for an MT-BS link that is shadowed by two different blockers is obtained as the sum of the two individual losses.

C. RF Lab Measurements

Besides these two main approaches, the attenuation profile could be taking from real measurements and applied for all blockers. Experimental work was carried out in an anechoic chamber at Heriot-Watt University where a rectangular copper sheet was placed exactly between two horn antennas, one for the transmitter and one for the receiver, separated by a distance $r = 2$ m. A narrowband measurement was performed, where the frequency was 28 GHz, and the transmitted power was 1 W. The transmitter and the receiver locations were fixed, and the copper sheet was placed in the middle to block the direct path between the transmitter and the receiver. The blocker was moved over several steps from right to left crossing the direct LOS path between the transmitter and the receiver. At each blocker position, the measurement of the resulting attenuation was collected, as presented in Fig. 3. We observed that the location of the blocker plays an important role in the resulting attenuation. The loss equation of the 3GPP blockage model for the same copper blocker is used, and this led to a similar finding. This RF lab measurements could be used as an attenuation profile and adopted as another blocker model.

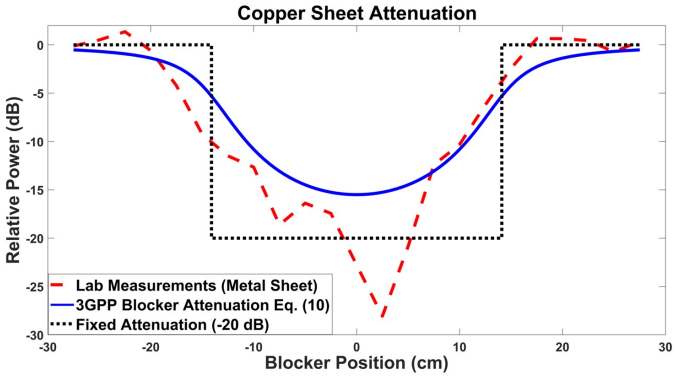

Fig. 3. Lab-measurement - Attenuation caused by a rectangular copper sheet.

IV. Methods to Model Blockages in Computer Simulation

For the mmWave band, modelling the blockage effect in open environments can be done in one of several ways listed in decreasing order of complexity: 1- full commercial ray tracing; 2- simplified geometric model; 3- Markov chain model [26]; or 4- the newly proposed sum of MC model. Although the performance of the first option is most realistic, where all the possible rays between the BS-RX are considered, the high complexity and time-required do not make it the preferred option, so it is out of this paper's scope. In this section, the simplified geometric and Markov chain models are introduced. They will be used for comparison later in this paper with the novel sum of MC model, which is presented in the next section, Section V. Two tasks are required for each model, the first is to determine the average number of blockers of a given environment, and secondly to compute the resulting attenuation. These results, finally, are considered in the received power calculations (8) to obtain the overall channel capacity results (9) for each model.

A. The Geometric Model

1) The Average Number of Blockers: Modelling blockage using a simplified geometric model comes with adequate performance and moderate complexity. The key factor that changes the average number of blockers is the number of blockers that cross the LOS path. However, this number increases with the BS-MT distance as in (3). As stated in [39], the longer the path, the more blockers would block it on average. The geometric model used in this paper was created in MATLAB for three different scenarios to represent different environments, as shown in Fig. 4. In each scenario, the mobile transceiver (MT) would move around the BS following a different receiver trajectory: circular, straight-line and sinusoidal shape. It is important to emphasize that the average number of blockers is not affected by the trajectory itself, but by the BS-MT distance. As explained in Section V, N equally spaced sample points are laid along these tracks. Once the MT starts moving and comes across each sample point, the number of blockers that block the LOS path between the mobile transceiver and the BS are computed using ray optics and stored in a vector with dimension N which is

completed once the MT reaches the last sample point along the track at sample time t_N. Running the simulation repeatedly with M Monte Carlo runs results in an $M \times N$ average number of blockers matrix, which contains the number of effective blockers at each sample points. The receiver's track scenarios as follows:

1) **Circular-shape Scenario:** In this scenario, the BS is in the centre of a circle and the receiver track follows the circle circumference as in Fig. 4(a). The purpose of having a circular track, where the distance to the base station is the same, r, is to keep the same average number of blockers at all sample locations, i.e. the average number of blockers in (3) will be $N_G^{'} = K_1$ where K_1 is a constant. This is a statistically stationary scenario.

2) **Straight-line shape Scenario:** In this scenario, there is a mobile transceiver that is moving along a straight track and passing by the base station, as shown in Fig. 4(b). Unlike the previous scenario, the average number of blockers here varies as the MT moves along the track based on the BS-MT distance; i.e. the average number of blockers in (3) will be $N_G^{'} = K_2 \times X_{infl}$ where K_2 is a constant and X_{infl} varies along the track and obtained using (2).

3) **Sinusoidal-shape Scenario:** The receiver track here has a sinusoidal shape as in Fig. 4(c), which is more complicated than the previous two cases, and it causes the average number of blockers to change with the MT location. In real-world scenarios, the MT could move around the BS at any distance and in any direction, so the BS-MT distance will keep changing. A good way to capture such fluctuations in simulation is to use a sinusoidal-shape scenario where the BS-MT distance keeps changing.

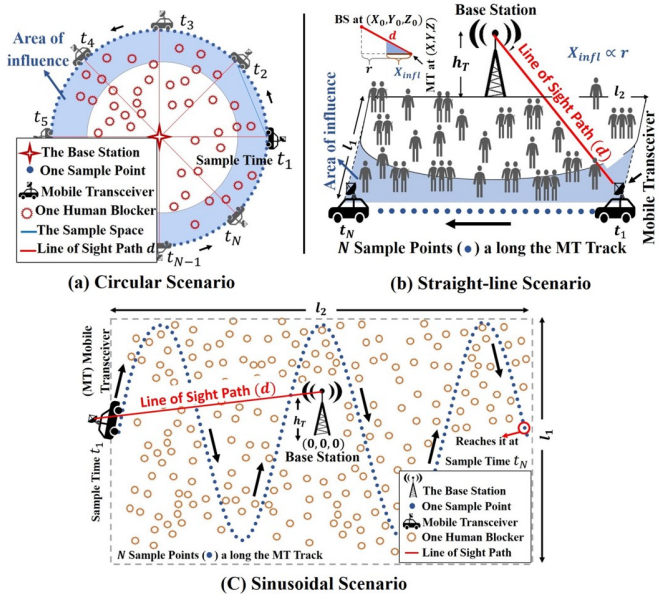

Fig. 4. Scenarios of the Geometric Model.

2) Blockage Attenuation: As mentioned in the previous section; two approaches to compute blockage attenuations are considered. First, when each human blocker causes a 20 dB fixed attenuation value, the overall resulting attenuation along the MT track is computed by multiplying the number of blockers by 20 dB. However, for 3GPP blockage approach, each blocker in the geometric model will be treated separately. As explained in Section III-B, at any sample point, whenever the LOS path intersects with a blocker, equation (10) is applied to calculate the attenuation value at this point.

3) Complexity Order of the Geometric Model: Assume that an MT moves around a BS within an area A_T. There are N_{BL} blockers within this area and N sample points. At each sample point, first, we need to check whether any one of the N_{BL} blockers crosses the LOS path. Then, if K blockers do cross the LOS path, we need to compute the 3GPP blockage attenuation equation for each blocker. For simplicity, we define the complexity of the 3GPP equation as requiring G operations. To carry out a Monte Carlo simulation, the model should be run M times. Thus, the complexity order is as follows:

$$\mathcal{O}(NN_{BL}MKG) \tag{12}$$

B. Markov Chain Model

As proposed in the previous study [26], the average number of blockers surrounding a moving transceiver could be captured using a Markov chain model with sufficient states to represent all possible numbers of blockers that could be expected. Each state represents the case where a specified number of blockers intersect the LOS path. The transition probability, P_{jk}, from state j to state k is defined by:

$$P_{jk} = \frac{n_{jk}}{\sum_{l=1}^{m} n_{jl}} \tag{13}$$

where n_{jk} is the number of times the average number of blockers changes from state j to state k along the track and m is the number of possible states. These transition probabilities between these states are obtained from running the geometric model offline and these probabilities are the only input needed for the Markov chain model for a given environment.

The Markov chain model works very well in a stationary scenario where the average number of blockers remains at the same level as in a circular-track scenario. For non-stationary scenarios, a single Markov chain can not model the change in the average number of blockers. In our initial work [26], we proposed a solution by dividing the receiver track into several sectors and representing each sector with a different Markov chain based on a different transition probability matrix.

Although the existing Markov chain model exhibits very good performance and it has very low complexity, it does have some limitations:

1) for non-stationary scenarios, dividing the receiver track into sectors is required and this is not easily automated.
2) Obtaining closed form results for the transition probability matrix is complex, especially for high average number of blockers cases. For these cases, the only practical option is to feed in the transition probability matrix from simulations of the geometric model.

3) This model works very well with the assumption that it has a fixed attenuation blocker when the total attenuation is simply the fixed value (e.g. 20 dB) multiplied by the number of blockers, but it is difficult to adapt if the attenuation value changes due to the blocker's location and orientation.

These limitations encourage us to develop a more flexible model that maintains the advantages of the Markov chain model and overcomes the limitations described above.

V. Sum of Markov Chains Model

A. Introducing the model

The sum of Markov chains (sum of MC) model can capture the average number of blockers surrounding a moving vehicle in a very efficient way using only basic knowledge about the surrounding environment. The fundamental idea of the model is as follows: having several Markov chains in parallel with a very limited number of states will successfully capture the average number of blockers for any given receiver track. The sum of MC model is based on the Binomial distribution, and it is constructed from several n chains in parallel, where each chain has only two states: state S_0, i.e. a clear LOS path, and state S_1, i.e. blocked by one blocker. The LOS path status converts from S_0 to S_1 using the probability P_{01}. Then, it remains in this state for l_B sample points until the mobile transceiver passes this blocker. Once this condition is met, it switches back to S_0, as shown in Fig. 5.

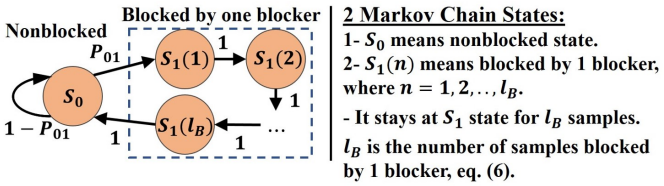

Fig. 5. Two Markov Chain Model states for one chain of the sum of MC.

The diagram in Fig. 6 explains the sum of MC model process. Each chain is treated as an independent event and has no impact on any other chain (i.e. independent probabilities). Moreover, the values of the probabilities, P_{01} is the same across all parallel chains. By making the right choice of P_{01} with enough number of chains, the sum of MC model will be able to predict an accurate value for the average number of blockers $N_S^{'}$ for a given environment.

The main advantage of the sum of MC model is its ability to work successfully with any receiver track scenario, whether it is stationary or non-stationary. For each chain in non-stationary scenarios, such as straight-line and sinusoidal, the input probability P_{01} will vary along the track so it is able to produce the required average number of blockers. The average number of blockers of the sum of MC for a given environment can be obtained using two different approaches: analytically and by simulation.

B. Analytical Calculation of Average Number of Blockers

This approach aims to obtain $N_S^{'}$ analytically from the input transition probability P_{01}. This can be done through several steps: first, the input transition probability needs to be modified. After that, we obtain the probability of a sample point along the chain being blocked by one blocker P_B. Then, the last step before computing the average number of blockers is to obtain the probabilities of having k blockers in a row.

1) The Transition Probability P_{01}: In the Markov chain model [26], the transition probability from state 0 (non-blocked state) to state 1 (blocked by one blocker) is:

$$P_{01} = \frac{\text{Number of Blockers}}{\text{Number of Sample Points}} \tag{14}$$

This definition is only applicable when the size of the blocker is small enough that it can block only one sample point at a time. However, in most practical cases, a blocker's shadow, as in Fig. 1(b), will cover several sample points, l_B, especially when the sample space between these points is quite small compared to the size of the blocker. Therefore, we need to redefine the transition probability and make it applicable to any blocker size and any sample space.

To modify (14), we split the sample points into two categories: blocked samples and non-blocked samples. Assuming all blockers have the same size, the total number of blocked samples is the number of samples blocked by one blocker multiplied by the total number of blockers. The total number of BL-blocked samples is computed similarly. Now, the modified transition probability, denoted as P_S, can be written as follows:

$$P_S = \frac{\text{No. of Blockers}}{\text{No. of Blockers} \times (\text{l}_{\text{NB}} + \text{l}_{\text{B}})} \Rightarrow P_S = \frac{1}{(l_{NB} + l_B)} \tag{15}$$

where the scalar l_B is the number of sample points that are shadowed by one blocker, which can be computed using (6). The scalar l_{NB} is the number of non-blocked samples before each blocker, and it is obtained from the ratio between the two transition probabilities that comes out of non-blocked state, as in Fig. 5, which is written as follows:

$$l_{NB} = \frac{1 - P_{01}}{P_{01}} \quad \text{(Sample Points)} \tag{16}$$

Now, we need to rewrite the modified transition probability P_S as a function of the original transition probability P_{01}, since P_{01} is still the main input. This is obtained by inserting (16) into (15) as follows:

$$P_S = \left(\frac{1 - P_{01}}{P_{01}} + l_B\right)^{-1} = \left(\frac{1}{P_{01}} - 1 + l_B\right)^{-1} \tag{17}$$

Having the modified transition probability in hand, now we can continue to calculate the average number of blockers $N_S^{'}$.

2) The Probability of being Blocked P_B: In each chain in the sum of MC model, the probability of a sample point being blocked by one blocker, P_B, is calculated as:

$$P_B = l_B P_S = l_B \left(\frac{1}{P_{01}} - 1 + l_B\right)^{-1} \tag{18}$$

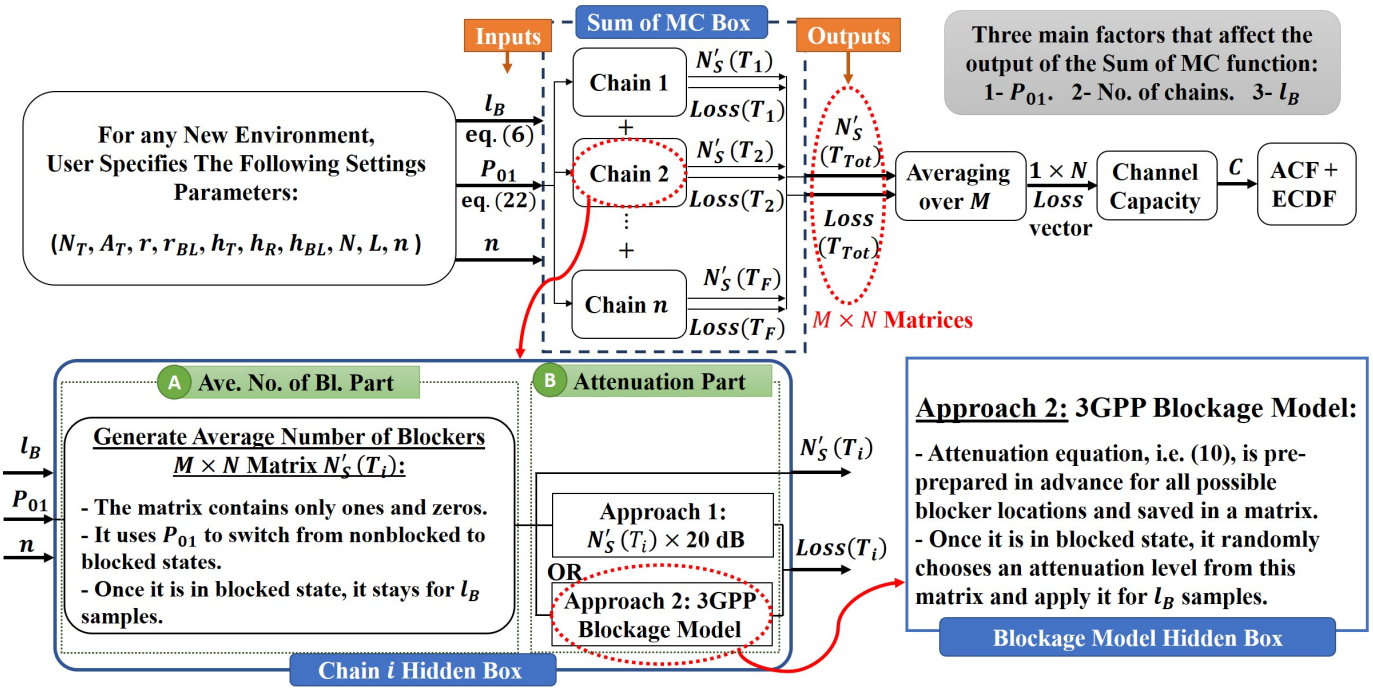

Fig. 6. Diagram explains the process of the sum of Markov Chains Model. (A link to the MATLAB code is available in Section VIII).

3) The Probabilities of Having k Blockers in a Row: Adding n two-state chains in parallel will result in 2^n outcomes that produce $(n+1)$ possible blockers in the range from $k=0$ up to n blockers. The probability of having k blockers in a row is expressed as:

$$P_k = (P_B)^k (1-P_B)^{n-k} {}^nC_k \tag{19}$$

where ${}^nC_k$ is the Binomial coefficient. Summing the probabilities for all k should equal one.

4) Average Number of Blockers N'_S: The average number of blockers of the sum of MC model is simply the mean of the Binomial distribution, and it is defined as follows:

$$N'_S = \mathbb{E}(K) = \sum_{k=0}^{k=n} kP_k = \sum_{k=0}^{k=n} k\binom{n}{k} {P_B}^k (1-P_B)^{n-k} \tag{20}$$

Using the well-known closed form of the Binomial distribution, the average number of blockers could be simplified further [40]:

$$N'_S = nP_B = nl_B \left(\frac{1}{P_{01}} - 1 + l_B\right)^{-1} \tag{21}$$

In principle, the average number of blockers in (21) and (3) should be equal, i.e. $N'_S \simeq N'_G$. The variable l_B is the average number of sample points that is affected by one blocker, which is obtained in (6). The transition probability P_{01} is the main input for the above function, which means each value of P_{01} will produce a corresponding average number of blockers, N'_S. To make the model adaptive to any scenario, we update the probability P_{01} at each sample point, based on how far the MT sample point is from the BS. We will have P_{01} vector of length N. Thus, from (21) we can define the optimal

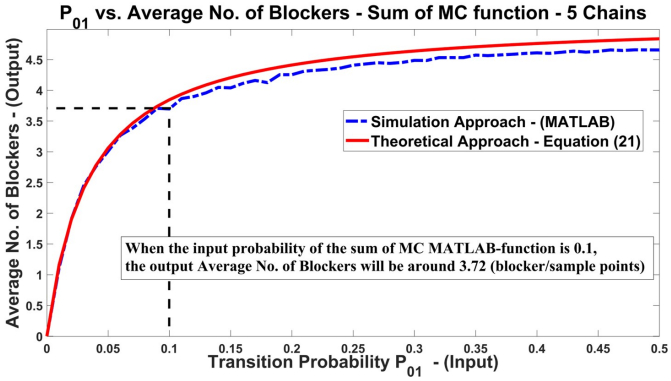

Fig. 7. The relationship's curve between the input P_{01} and the output N'_S of the sum of MC function, where $l_B = 30$ and $n = 5$.

transition probability that leads to the desired average number of blockers as follows:

$$P_{01} = \left(\frac{nl_B}{N'_G} + 1 - l_B\right) \tag{22}$$

C. Average Number of Blockers by Simulation

A MATLAB function was created that takes the transition probability P_{01} as an input and give the average number of blockers of the sum of MC model as an output as shown in Fig.6. To understand the relationship between the input P_{01} and the output N'_S of the sum of MC function, we plotted the probability versus the output average number of blockers N'_S in Fig. 7. Note, due to the sparse distribution of blockers, there is no need for very high values of the transition probability. This curve is a result of combining five chains. Fig.7 could

be used as a lookup table and guidance for the sum of MC function.

D. Blockage Attenuation

As explained in Section III, two approaches are considered for blockage attenuation as presented in Fig.6. For the fixed-attenuation scenario, whenever there is a human blocker, a 20 dB loss is added. As noted in Section II-A, the attenuation of the model is simply computed by multiplying the number of blockers by 20 dB, e.g. if the LOS path blocked by 2 blockers, the resulting attenuation is 20 dB + 20 dB = 40 dB. The second approach is the 3GPP blockage scenario. To avoid computation at each time we run the sum of MC function, the attenuation equation (10) of the 3GPP blockage model is computed in advance for all possible locations along the direct line between BS and MT and saved as attenuation levels in a lookup table within a hidden MATLAB function. Thus, at any chain of the sum of MC model, whenever the signal status changes to a blocked state, the hidden MATLAB function will choose randomly one of the attenuation levels and apply it keep it running for l_B sample points until the status switches back to the non-blocked state. However, the sum of MC model can equally be applied to any other blockage model, which can be easy used instead of the 3GPP blockage model.

The next step entails inserting these attenuation losses into the calculation of the received power. Then, the overall average channel capacity for this model is computed using (9).

E. Complexity Order of the Adaptive Sum of MC Model:

The 3GPP blockage model here is computed offline for all possible locations, as mentioned in the above subsection, so it will not introduce any further complexity to the sum of MC model. Likewise, the transition probability P_{01} vector is computed offline as well. The complexity order of the sum of MC model is as follows:

$$\mathcal{O}(nNM) \tag{23}$$

where n is the number of chains which is usually a small number, e.g. for all our scenarios, $n \leq 5$. The variables N and M are the number of sample points, and the number of Monte Carlo runs respectively. Thus, it is obvious that the proposed sum of MC model is significantly less complex than the geometric model, i.e. (12).

VI. Results and Discussions

All the three models – geometric, Markov chain and the sum of MC- aim to capture the dynamic of the blockers and to investigate the effect of the resulting attenuation on the LOS link in mmWave communication systems. The proposed sum of MC model is computationally efficient. For instance, in the sinusoidal-shape track, which is a complicated non-stationary scenario, we observe that the run-time of the sum of MC model is 7000 times less than the run-time of the geometric model. In this section, the overall average channel capacity (9) along the receiver track is key to the comparison between the models. Moreover, the autocorrelation function (ACF) in (24) and the empirical cumulative distribution function (ECDF) in (25) of the average capacity $C(t)$ are used as comparison metrics.

$$ACF(\Delta t) = \mathbb{E}[C(t)C(t+\Delta t)] \tag{24}$$

$$ECDF(c(t)) = P(C \leqslant c(t)) \tag{25}$$

Table I specifies all the parameters used in the simulation scenarios. In the following subsections, the results of all the three models – geometric, Markov chain and the sum of MC – are presented based on the receiver track scenarios; i.e. stationary scenario (circular-shape track), non-stationary scenarios (straight-line and sinusoidal-shape tracks). Moreover, to show how the sum of MC model can apply any attenuation function, the results of integrating the attenuation profile of the lab measurements, see Section III-C, is presented in the last subsection of the discussion.

TABLE I
System and Antenna Parameters

General Settings			
BS Power	$P_T(Total) = 1$ W	BS height	$h_T = 2.5$ m
Noise Power	$N_O = -123.91$ dB	MT height	$h_R = 1.5$ m
Bandwidth	100 MHz	Blocker dimension	$r_{BL} = 0.235$ [22] $h_{BL} = 1.8$ (m)
Carrier Freq.	$f_c = 30$ GHz	D_T, D_R in (7)&(8)	8 Dipole antennas
The Circular Scenario		**The Straight-line Scenario**	
Sample points	$N = 360$	No. of Sample (points & space)	$N = 34001,\ \lambda/2$
No. of runs	$M = 100$	No. of runs	$M = 100$
Tot. No. of BL	$(10, 50, 100, 200, 500)$	Tot. No. of BL	$N_{BL} = 50$
Circ. Radius r	$(10, 15, 20, 25, 30)$m	A_T dim. (m)	$l_1 = 15, l_2 = 170$
The Sinusoidal Scenario		**RF Lab Settings**	
Sample points	$N = 500$	BS Power	$P_T(Total) = 1$ W
No. of runs	$M = 500$	Carrier Freq.	$f_c = 28$ GHz
Tot. No. of BL	$N_{BL} = 200$	BS, MT (Height) and BS-MT Dist.	$h_T = 1, h_R = 1(m)$ $r = 2$ (m)
A_T dim. (m)	$l_1 = 16, l_2 = 24$	Blocker dimension	$l_{B1} = 0.36$ (m) $l_{B2} = 0.282$ (m)

A. Stationary Scenario: Circular-track Comparisons

The results of the stationary circular-track scenario, see in Fig. 4(a) in subsection IV-A1-(a), are presented based on the type of the blocker; i.e. fixed attenuation or 3GPP blocker.

1) Fixed Attenuation Blocker Results: In the case of the fixed attenuation blocker, see Section III-A, there is no need to compute the attenuation value caused by each blocker separately, so the Markov chain model works here with no problem. Thus, both the Markov chain and the sum of MC models work very well, and they match well with the geometric model.

The three models; geometric, Markov chain, and sum of MC; can be compared by the average number of blockers they produce. Table II shows the histogram by a percentage of the number of blockers that intersect with the LOS path. All models show a good match with each other in the overall average number of blockers with only slight variations. The small MSE value of 0.19 between the histogram of geometric and sum of MC models reflects the accuracy of the sum of MC model in capturing the average number of blockers. One of the advantages of the sum of MC over the Markov chain is that the average number of blockers can be mathematically found easily using (21), which has a very good match with the simulation results, as shown in Table II.

TABLE II

AVERAGE NUMBER OF BLOCKERS $N^{'}$ COMPARISON BETWEEN THE THREE MODELS: 1) GEOMETRIC MODEL (BY SIMULATION AND THEORETICALLY), 2) MARKOV CHAIN MODEL, AND 3) THE SUM OF MC MODEL (BY SIMULATION AND THEORETICALLY) - FIXED ATTENUATION BLOCKAGE MODEL

Percentage of the Histogram of Average Number of Blockers %								The Average Number of Blockers $N^{'}$	Reference Section of The Paper
Blockage Model Name & Approach		Number of blockers intersecting with LOS path					MSE with Geometric Sim.		
		0	1	2	3	4	5		
(1) Geometric	Theoretically	43.68	39.35	14.18	2.55	0.23	0.00008	0.26	0.732	II (3)&V-B (19)
	Simulation	44.35	39.92	13.4	2.14	0.16	0.028	0	0.738	IV-A
(2) Markov Chain	Simulation	43.18	40.31	14.39	1.97	0.14	0.0056	0.42	0.755	IV-B
(3) Sum of MC	Theoretically	44.85	39	13.57	2.36	0.2	0.0071	0.19	0.74	V-B ((19)&(21))
	Simulation	46.36	38.18	13.03	2.18	0.24	0.0056	1.2	0.71	V-C

TABLE III

OVERALL CHANNEL CAPACITY C & AVERAGE NUMBER OF BLOCKERS $N^{'}$ COMPARISON BETWEEN THE THREE MODELS: 1) GEOMETRIC, 2) MARKOV CHAIN (MC) MODEL, AND 3) SUM OF MC - TWO CIRCULAR SHAPE SCENARIOS BOTH WITH FIXED ATTENUATION BLOCKAGE MODEL

The Overall Average Capacity Along all the Circle Track (bits/s/Hz) & Average Number of Blockers (BL) $N^{'}$									
Circle Scenario 1 (Vary No. of Blockers & Fixed Circle Radius) - Circle Radius is r =10 (m), 360 Sample Points									
N_{BL} Total No. of BL in the Area	(1) Geometric Model		(2) MC Model		(3) Sum of MC Model				
	Channel Capacity	Average No. of BL $N^{'}$	Channel Capacity	Average No. of BL $N^{'}$	Channel Capacity	Average No. of BL $N^{'}$	No. of MC Chains	P_{01}	l_B No. of blocked samples by one BL
10	13.67	0.037	13.68	0.036	13.66	0.038	1	0.01	4
50	12.7	0.188	12.69	0.189	12.72	0.184	2	0.025	4
100	11.51	0.37	11.52	0.369	11.53	0.367	4	0.025	4
200	9.1	0.738	8.99	0.755	9.24	0.717	5	0.042	4
500	2.17	1.848	2.13	1.855	2.26	1.832	5	0.144	4
Circle Scenario 2 (Fixed No. of Blockers & Vary Circle Radius) - Number of Blockers in the Area is $N_{BL} = 200$ (Blockers), 360 Sample Points									
Radius r (m)	(1) Geometric Model		(2) MC Model		(3) Sum of MC Model				
	Channel Capacity	Average No. of BL $N^{'}$	Channel Capacity	Average No. of BL $N^{'}$	Channel Capacity	Average No. of BL $N^{'}$	No. of MC Chains	P_{01}	l_B No. of blocked samples by one BL
10	9.1	0.738	8.99	0.755	9.24	0.717	5	0.042	4
15	9.54	0.492	9.58	0.487	9.46	0.504	4	0.048	3
20	9.58	0.361	9.62	0.355	9.57	0.363	3	0.068	2
25	9.4	0.287	9.41	0.288	9.42	0.287	2	0.085	2
30	9.21	0.237	9.24	0.233	9.20	0.238	1	0.155	2

Table III shows the overall channel capacity comparison of two circular shape scenarios, both with the fixed attenuation blockage model. The first scenario shows that by fixing the whole area and increasing the number of blockers within this area, the overall channel capacity drop. Both Markov chain and the sum of MC models work very well when compared with the geometric model. For instance, the difference in the capacity results of the two models compared with the geometric one is only 0.01 (bits/s/Hz) when the number of existing blockers is 10. The models yield equally close results for 100 blockers. The second part of the table shows the capacity comparison as well, but here the total number of blockers is fixed, i.e. 200, and the BS-MT distance r, varies. The capacity results of both Markov chain and the sum of MC models match the geometric results very well with very small errors. For example, when $r = 30$ m, the capacity result of the sum of MC is only 0.01 (bits/s/Hz) higher than the geometric while the capacity result of the Markov chain is only 0.03 (bits/s/Hz) higher.

Fig. 8 and Fig. 9 respectively show the average ACF and the ECDF of the channel capacity. Both Markov chain and the sum of MC models work very well, and they match well with the geometric curve. Regarding the sum of MC model, the sum of 5 chains was used to produce the required average number of blockers. The input value of P_{01} for the MATLAB function is 0.042, and it is fixed all over the track. However,

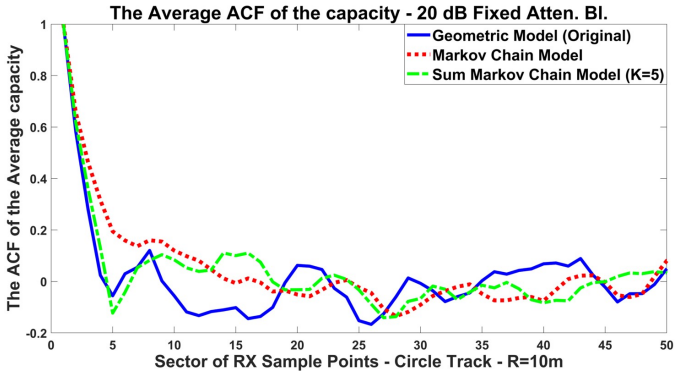

Fig. 8. Average ACF of the Capacity of the circular track, r=10m, with No. of BL=200, 360 sample points, and M=100 runs - Fixed Attenuation.

the desired average number of blockers can also be achieved, by a different number of summed chains, but that should be with the right choice of P_{01}. In Fig. 8, the average ACF of the capacity shows a better match with the geometric for the sum of MC than the Markov chain model. However, Fig. 9 shows that both models match the geometric curve very well.

2) 3GPP Blocker Results: It is more practical to use an attenuation value caused by a blocker model that varies based on the location and orientation of the blocker; such as the 3GPP blocker model in Section III-B. The Markov chain model

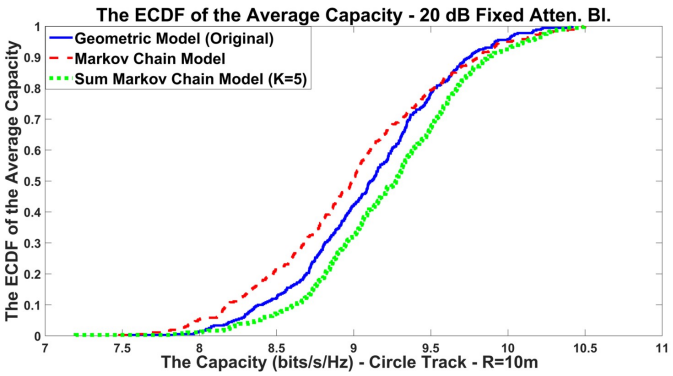

Fig. 9. The ECDF of the Capacity of the circular track, r=10m, with No. of BL=200, 360 sample points, and M=100 runs - Fixed Attenuation.

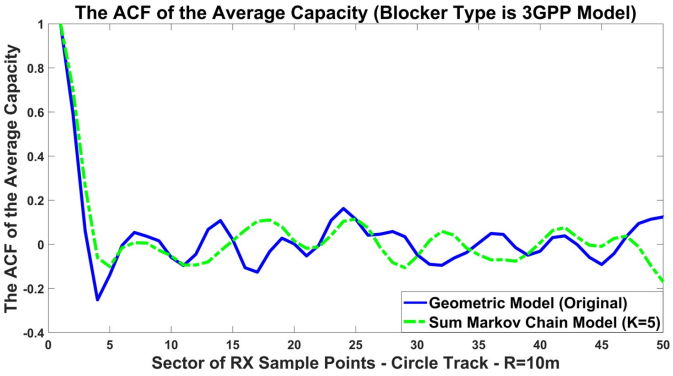

Fig. 10. Average ACF of the Capacity of the circular track, r=10m, with No. of BL=300, 360 sample points, and M=500 runs - 3GPP Blocker.

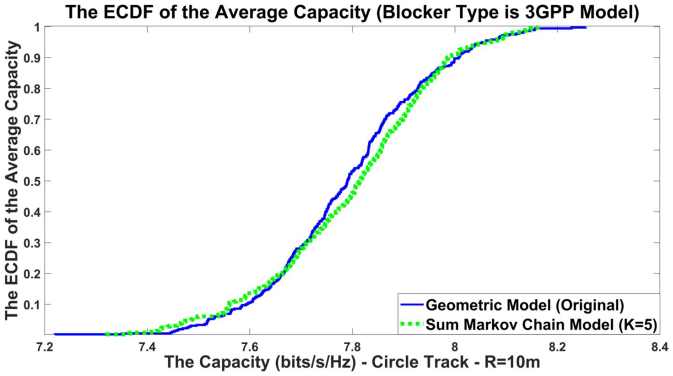

Fig. 11. The ECDF of the Capacity of the circular track, r=10m, with No. of BL=300, 360 sample points, and M=500 runs - 3GPP Blocker.

can not be easily modified to predict how much attenuation is caused by each blocker. Here, one of the advantages of the sum of MC emerges: it is flexible, and it can adopt any attenuation profile. As shown in Fig. 10 and Fig. 11, both the average ACF and ECDF of average capacity curves show that the performance of the sum of MC model is as good as that of the geometric model.

B. Non-stationary Scenario Comparisons

The sum of MC model has an adaptation feature that makes it applicable even to non-stationary scenarios such as straight-line and sinusoidal-shape tracks, where the average number

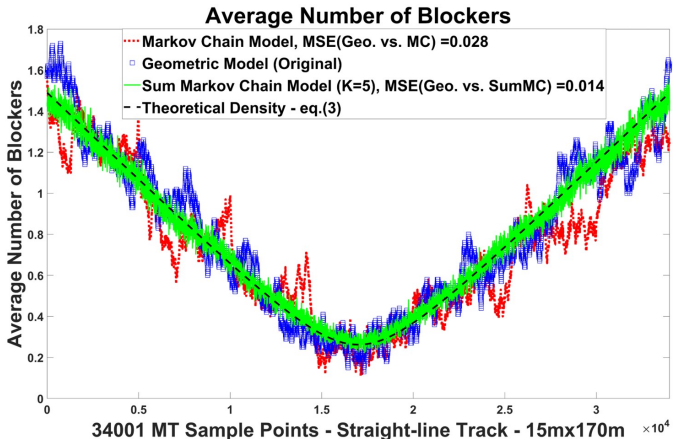

Fig. 12. Average number of blockers along the MT straight-line track with No. of BL=130, $r_{BL} = 0.235$m, 34001 MT sample points, sample space $\lambda/2$, and M=100 runs - Fixed Attenuation.

of blockers is not constant. This advantage is obtained by updating the input value P_{01} over time based on how far the MT sample point is from the BS. The optimal P_{01} values across all positions along the MT track are obtained from (22) and used as an input of the sum of Markov's MATLAB function. In this paper, we have introduced two non-stationary scenarios:

1) Straight-line Scenario: As mentioned in Section IV-A1-(b), in this scenario, the mobile transceiver is approaching and passing the BS. The track length, 170 m, is chosen to investigate the difference in the average number of blockers with distance. When it is far from the BS, it is more likely to suffer from more blockers blocking the LOS path, so $N_G^{'}$ in Fig. 12 starts high, then, it decreases until it reaches the minimum when the MT is very close to the BS. Then, it starts to rise again. The theoretical approach for computing the average number of blockers $N_G^{'}$ in (3) is matching the geometric-based simulation curve very well. Although the scenario is not stationary, the resulting $N_S^{'}$ curve of the sum of MC model in Fig. 12 matches the geometric curve very well. We used (22) to find the optimal transition probability vector P_{01} as input the sum of MC function. However, regarding the Markov chain model, i.e. the red curve, since the scenario is not stationary, it is required to have several chains based on multiple probability transition matrices to obtain the Markov chain results, as described in [26].

The average ACF curve of the sum of MC in Fig. 13 has a perfect match with the geometric curve. Both the sum of MC and the Markov chains curves match very well, but the sum of MC curve has a slightly better performance. The ECDF of the average channel capacity in Fig. 14 shows that although all models perform closely, the sum of MC curve fits better to the geometric curve than the Markov chain curve.

2) Sinusoidal Scenario: This sinusoidal-shape track is even more complicated than the straight-line scenario. As mentioned in subsection IV-A1-(c), and as shown in Fig. 4(c), the mobile transceiver is moving along a cosine track, while the BS is at the origin point. In this scenario, the distance between

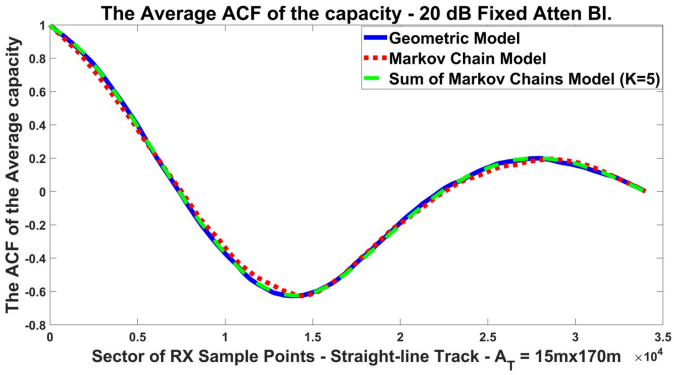

Fig. 13. The Average ACF of the Capacity of the straight-line track with No. of BL=130, $r_{BL} = 0.235$m, 34001 MT sample points, sample space $\lambda/2$, and M=100 runs - Fixed Attenuation.

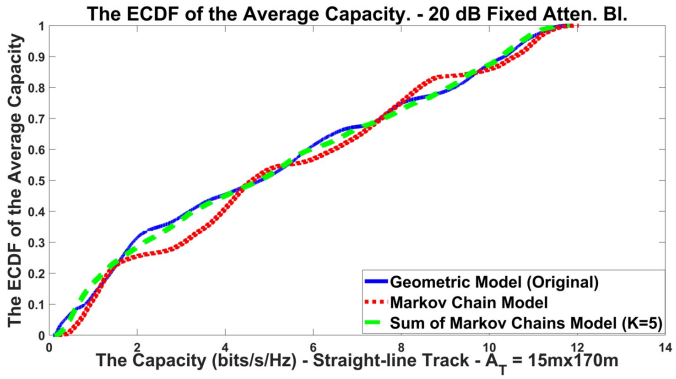

Fig. 14. The ECDF of the Capacity of the straight-line track with No. of BL=130, $r_{BL} = 0.235$m, 34001 MT sample points, sample space $\lambda/2$, and M=100 runs - Fixed Attenuation.

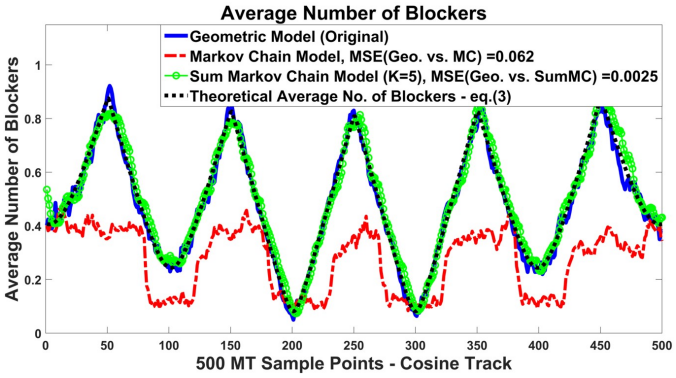

Fig. 15. Average number of blockers along the MT Cosine-shape track with No. of BL=200, $r_{BL} = 0.2821$m, 500 sample points, and M=500 runs - Fixed Attenuation.

the BS and MT increases and decreases repeatedly, hence the average number of blockers fluctuates as well. This is a severe and quite complicated non-stationary case. By following the simulation approach mentioned in Section V-C, the output $N_S^{'}$ of the sum of MC function show a perfect fit with the geometric average number of blockers in Fig. 15. However, due to the complexity of the scenario, the Markov chain model fails to adapt even with the use of multiple sectors idea [26]. We have divided the track into 9 sectors which are based on only two Markov chains: one for the peaks and bottoms of the curve, and one for the straight lines.

Both ACF and ECDF channel capacity curves of the sum of MC model, in Fig. 16 and Fig. 17 sequentially, are showing an identical match with the geometric curve. Although we use several chains for different segments, the Markov chain model fails to adapt to this severe case of non-stationary scenario, as is obvious from the results in Fig. 16 and Fig. 17. These figures show the benefit of the proposed sum of MC model.

Discussion: In a more general trajectory, three main factors that affect the average number of blockers: 1) The BS-MT distance. 2) The blocker width. 3) The heights of the BS, MT, and the blocker. The results show that the adaptive sum of MC model can successfully update the average number of blockers by adjusting the number of blockers based on the BS-MT distance through increasing or decreasing the number of chains n and the transition probabilities P_{01}.

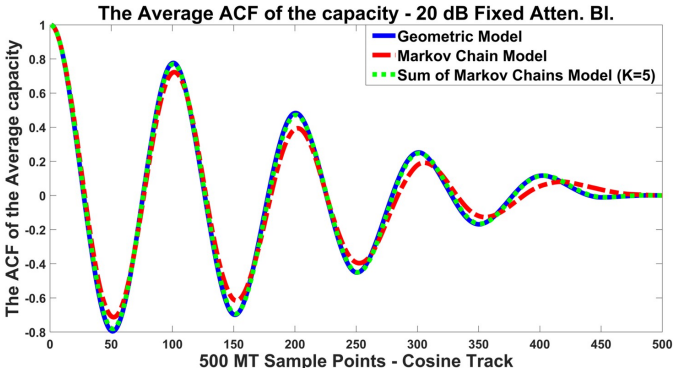

Fig. 16. The Average ACF of the Capacity of the Cosine track with No. of BL=200, $r_{BL} = 0.2821$m, 500 sample points, and M=500 runs - Fixed Attenuation.

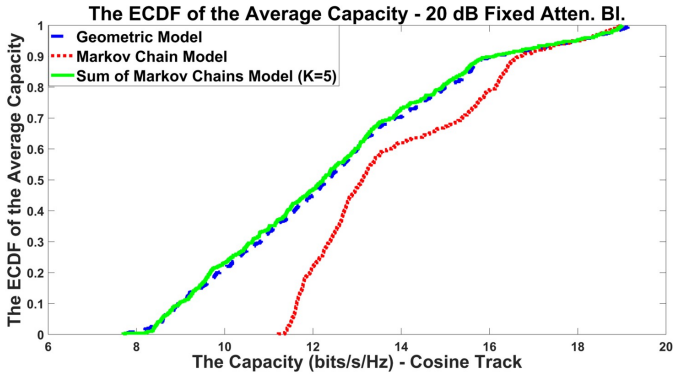

Fig. 17. The ECDF of the Capacity of the Cosine track with No. of BL=200, $r_{BL} = 0.2821$m, 500 sample points, and M=500 runs - Fixed Attenuation.

C. Results of Integrating Lab measurements into the Sum of MC Model

The novel sum of MC model can integrate any attenuation profile. Clearly, from the previous results in Section VI-A2, it has adopted the 3GPP blockage model successfully. To test this feature furthermore, the attenuation profile of the copper sheet taken from the lab measurements, see Section III-C,

is integrated with the sum of MC function. To compare the results we have created a circular geometric model with the following parameters: ($r = 2$m, blockers are placed 1 m from the BS i.e. in the middle, $r_{BL} = 0.14$, 4 copper-sheet blockers, $N = 360$ sample points, and $h_{BL} = h_R = h_T = 1$ m), which are similar to the lab sittings in Table I. Due to the copper sheet size and location, the number of blocked samples for one blocker is $l_B = 17$ samples. The resulting overall average of the channel capacity (9) of the sum of MC is $C = 17.67$ (bits/s/Hz), which is very close to the average channel capacity obtained from the geometric model $C = 17.85$ (bits/s/Hz). This accuracy and adaptation of any attenuation profile reflect the novelty of the proposed sum of MC model.

VII. Conclusion

A novel sum of Markov chains model that successfully captures the dynamics of blockers surrounding a moving transceiver in both stationary and non-stationary scenarios is described. Compared with a baseline geometric model, both the sum of MC and Markov chains models are computationally efficient. We found that the run-time of the sum of MC is three orders of magnitude less than the geometric model for a severe non-stationary scenario. The proposed sum of MC model has further advantages, which overcome the drawbacks of the Markov chain method. These are: 1) It is adaptive for any non-stationary scenario with no additional effort. 2) The ability to integrate any attenuation function; including the 3GPP blockage model, and any lab-measurement attenuation profile. 3) Unlike the Markov chain model, the mathematical derivation of the average number of blockers can be found in closed form. All the average channel capacity results and the curves of both ECDF and ACF show good performance for the sum of MC compared with the geometric model. We believe that this computationally efficient sum of MC is valuable for evaluating high gain beam pattern techniques for directional mmWave communication systems. For future work, evaluating beam training algorithms with the proposed blockage model will be investigated. Moreover, instead of operating only on the direct LOS path, the sum of MC blockage model can easily be extended to apply to multipath scenarios. Each path would be treated independently; unless there is a correlation between the paths. Although the proposed sum of MC model serves the V2I system, the model can also be modified to apply for more general models, such as vehicle-to-everything (V2X) systems.

VIII. Software

The MATLAB code used for the proposed sum of Markov chains model is available from the link below:

https://datashare.is.ed.ac.uk/handle/10283/3657

Acknowledgement

F. Alsaleem gratefully acknowledges funding his PhD studies by Qassim University, Qassim, Saudi Arabia.

The authors are grateful to Cristian Alistarh, a PhD candidate at Heriot-Watt University, and his supervisor: Dr Symon Podilchak for allowing access to Heriot-Watt University's RF lab, and for their great help in setting and taking the measurements reported in Fig. 3.

References

[1] P. B. Papazian, G. A. Hufford, R. J. Achatz, and R. Hoffman, "Study of the local multipoint distribution service radio channel," *IEEE Transactions on Broadcasting*, vol. 43, no. 2, pp. 175–184, 1997.

[2] S. Salous *et al.*, "Millimeter-wave propagation: Characterization and modeling toward fifth-generation systems. [wireless corner]," *IEEE Antennas and Propagation Magazine*, vol. 58, no. 6, pp. 115–127, December 2016.

[3] Y. Niu, Y. Li, D. Jin, L. Su, and A. Vasilakos, "A survey of millimeter wave (mmWave) communications for 5G: Opportunities and challenges," *Wireless Networks*, vol. 21, no. 8, pp. 2657–2676, 2015.

[4] J. S. Lu, D. Steinbach, P. Cabrol, and P. Pietraski, "Modeling human blockers in millimeter wave radio links," *ZTE communications*, vol. 10, no. 4, pp. 23–28, 2012.

[5] S. Singh *et al.*, "Blockage and directivity in 60 GHz wireless personal area networks: from cross-layer model to multihop MAC design," *IEEE Journal on Selected Areas in Communications*, vol. 27, no. 8, pp. 1400–1413, October 2009.

[6] C. Gustafson, K. Haneda, S. Wyne, and F. Tufvesson, "On mm-Wave multipath clustering and channel modeling," *IEEE Transactions on Antennas and Propagation*, vol. 62, no. 3, pp. 1445–1455, March 2014.

[7] S. Niknam, B. Natarajan, and R. Barazideh, "Interference analysis for finite-area 5G mmWave networks considering blockage effect," *IEEE Access*, vol. 6, pp. 23 470–23 479, 2018.

[8] M. Gapeyenko *et al.*, "On the temporal effects of mobile blockers in urban millimeter-wave cellular scenarios," *IEEE Transactions on Vehicular Technology*, vol. 66, no. 11, pp. 10 124–10 138, 2017.

[9] C. Slezak *et al.*, "Empirical effects of dynamic human-body blockage in 60 GHz communications," *IEEE Communications Magazine*, vol. 56, no. 12, pp. 60–66, December 2018.

[10] I. K. Jain, R. Kumar, and S. Panwar, "Driven by capacity or blockage? a millimeter wave blockage analysis," in *2018 30th International Teletraffic Congress (ITC 30)*, vol. 01, September 2018, pp. 153–159.

[11] I. K. Jain, R. Kumar, and S. S. Panwar, "The impact of mobile blockers on millimeter wave cellular systems," *IEEE Journal on Selected Areas in Communications*, vol. 37, no. 4, pp. 854–868, April 2019.

[12] V. Semkin *et al.*, "Estimation of optimum antenna configurations supported by realistic propagation models at 60 GHz," in *The 8th European Conference on Antennas and Propagation (EuCAP 2014)*, April 2014, pp. 3434–3438.

[13] V. Degli-Esposti *et al.*, "Ray-tracing-based mm-Wave beamforming assessment," *IEEE Access*, vol. 2, pp. 1314–1325, 2014.

[14] B. Han *et al.*, "A 3D human body blockage model for outdoor millimeter-wave cellular communication," *Physical Communication*, vol. 25, pp. 502–510, 2017.

[15] M. Gapeyenko *et al.*, "Spatially-consistent human body blockage modeling: A state generation procedure," *IEEE Transactions on Mobile Computing*, pp. 1–1, 2019.

[16] M. Abouelseoud and G. Charlton, "The effect of human blockage on the performance of millimeter-wave access link for outdoor coverage," in *2013 IEEE 77th Vehicular Technology Conference (VTC Spring)*, June 2013, pp. 1–5.

[17] M. Jacob *et al.*, "Extension and validation of the IEEE 802.11ad 60 GHz human blockage model," in *2013 7th European Conference on Antennas and Propagation (EuCAP)*, April 2013, pp. 2806–2810.

[18] M.Jacob *et al.*, "A ray tracing based stochastic human blockage model for the IEEE 802.11ad 60 GHz channel model," in *Proceedings of the 5th European Conference on Antennas and Propagation (EUCAP)*, April 2011, pp. 3084–3088.

[19] M. Jacob *et al.*, "Fundamental analyses of 60 GHz human blockage," in *2013 7th European Conference on Antennas and Propagation (EuCAP)*, April 2013, pp. 117–121.

[20] Y. Dalveren, A. H. Alabish, and A. Kara, "A simplified model for characterizing the effects of scattering objects and human body blocking indoor links at 28 GHz," *IEEE Access*, vol. 7, pp. 69 687–69 691, 2019.

[21] G. R. MacCartney, T. S. Rappaport, and S. Rangan, "Rapid fading due to human blockage in pedestrian crowds at 5G millimeter-wave frequencies," in *GLOBECOM 2017 - 2017 IEEE Global Communications Conference*, December 2017, pp. 1–7.

[22] G. R. MacCartney, S. Deng, S. Sun, and T. S. Rappaport, "Millimeter-wave human blockage at 73 GHz with a simple double knife-edge diffraction model and extension for directional antennas," in *2016 IEEE 84th Vehicular Technology Conference (VTC-Fall)*, September 2016, pp. 1–6.

[23] S. H. Aftabi Momo and M. Munjure Mowla, "Effect of human blockage on an outdoor mmWave channel for 5G communication networks," in *2019 22nd International Conference on Computer and Information Technology (ICCIT)*, 2019, pp. 1–6.

[24] W. Qi *et al.*, "Measurements and modeling of human blockage effects for multiple millimeter wave bands," in *2017 13th International Wireless Communications and Mobile Computing Conference (IWCMC)*, June 2017, pp. 1604–1609.

[25] M. Gapeyenko *et al.*, "Analysis of human-body blockage in urban millimeter-wave cellular communications," in *2016 IEEE International Conference on Communications (ICC)*, May 2016, pp. 1–7.

[26] F. Alsaleem, J. S. Thompson, and D. I. Laurenson, "Markov chain for modeling 3D blockage in mmWave V2I communications," in *2019 IEEE 89th Vehicular Technology Conference (VTC2019-Spring)*, April 2019, pp. 1–5.

[27] L. Raschkowski *et al.*, "METIS Channel Models (D1.4)," July 2015.

[28] "Study on channel model for frequency spectrum above 6 GHz (release 14)," *Technical Report TR 38.900, 3GPP*, 2017.

[29] J. S. Romero-Peña and N. Cardona, "Applicability limits of simplified human blockage models at 5G mm-Wave frequencies," in *2019 13th European Conference on Antennas and Propagation (EuCAP)*, March 2019, pp. 1–5.

[30] S. Dehnie, "Markov chain approximation of Rayeleigh fading channel," in *2007 IEEE International Conference on Signal Processing and Communications*, November 2007, pp. 1311–1314.

[31] I. Kashiwagi, T. Taga, and T. Imai, "Time-varying path-shadowing model for indoor populated environments," *IEEE Transactions on Vehicular Technology*, vol. 59, no. 1, pp. 16–28, January 2010.

[32] R. Ford *et al.*, "Markov channel-based performance analysis for millimeter wave mobile networks," in *2017 IEEE Wireless Communications and Networking Conference (WCNC)*, pp. 1–6.

[33] M. Boban, X. Gong, and W. Xu, "Modeling the evolution of line-of-sight blockage for V2V channels," in *2016 IEEE 84th (VTC-Fall) Conference*, pp. 1–7.

[34] T. S. Rappaport, R. W. Heath Jr, R. C. Daniels, and J. N. Murdock, *Millimeter wave wireless communications*. Pearson Education, 2015.

[35] A. K. Gupta, J. G. Andrews, and R. W. H. Jr, "Macro diversity in cellular networks with random blockages," 2017.

[36] D. C. Hogg, "Fun with the Friis free-space transmission formula," *IEEE Antennas and Propagation Mag.*, vol. 35, no. 4, pp. 33–35, 1993.

[37] P. Brémaud, "Shannon's capacity theorem. in: Discrete probability models and methods. probability theory and stochastic modelling," *Springer, Cham*, vol. 78, 2017.

[38] P. Mogensen *et al.*, "LTE capacity compared to the Shannon bound," in *2007 IEEE 65th Vehicular Technology Conference - VTC2007-Spring*, April 2007, pp. 1234–1238.

[39] T. Bai, R. Vaze, and R. W. Heath, "Analysis of blockage effects on urban cellular networks," *IEEE Transactions on Wireless Communications*, vol. 13, no. 9, pp. 5070–5083, 2014.

[40] Feldman, Joel. Joelfel's webpage. [Online]. Available: http://www.math.ubc.ca/~feldman/

Fahd Nasser Alsaleem received his Bachelor's degree in Communications and Electronics Engineering from Qassim University, Buraydah, Saudi Arabia, in 2011. Since then, he had been a Teaching Assistant at the College of Engineering, Unaizah, Qassim University. He received M.Sc. degree in Signal Processing and Communications from the University of Edinburgh, U.K., in 2016. From 2016-2020, he has been pursuing the PhD degree in Communications Engineering with the Institute for Digital Communications, University of Edinburgh, U.K. His research interests are in the area of mmWave Communications for 5G and beyond, and Blockage Modelling. After earning the PhD, Fahd is expected to be Assistant Professor at the College of Engineering, Qassim University, Saudi Arabia.

John S. Thompson (F'16) is currently a Professor at the School of Engineering in the University of Edinburgh. He specializes in antenna array processing, cooperative communications systems, energy efficient wireless communications and their applications. He has published in excess of three hundred and fifty papers on these topics. In 2018, he was the co-chair of the IEEE SmartGridComm conference held in Aalborg, Denmark. He currently participates in a UK research project which signal processing concepts for the information age. In January 2016, he was elevated to Fellow of the IEEE for contributions to antenna arrays and multi-hop communications. In 2015-2018, he has been recognised by Thomson Reuters as a highly cited researcher.

David I. Laurenson is currently a Reader at The University of Edinburgh, Scotland. His interests lie in mobile communications: at the link layer this includes measurements, analysis and modelling of channels and MAC protocols, whilst at the network layer this includes provision of mobility management and Quality of Service support. His research extends to practical implementation of wireless networks to other research fields, such as prediction of fire spread using wireless sensor networks, deployment of communication networks for distributed control of power distribution networks, and sensor networks for environmental monitoring and structural analysis.